

Formation, Reactivity, and Photorelease of Metal Bound Nitrosyl in $[\text{Ru}(\text{trpy})(\text{L})(\text{NO})]^{n+}$ (trpy = 2,2':6',2''-Terpyridine, L = 2-Phenylimidazo[4,5-f]1,10-phenanthroline)

Somnath Maji,[†] Biprajit Sarkar,[‡] Malay Patra,[†] Atanu Kumar Das,[‡] Shaikh M. Mobin,[†] Wolfgang Kaim,^{*,‡} and Goutam Kumar Lahiri^{*,†}

Department of Chemistry, Indian Institute of Technology—Bombay, Powai, Mumbai 400076, India, and Institut für Anorganische Chemie, Universität Stuttgart, Pfaffenwaldring 55, D-70550 Stuttgart, Germany

Received November 2, 2007

Nitrosyl complexes with $\{\text{Ru}-\text{NO}\}^6$ and $\{\text{Ru}-\text{NO}\}^7$ configurations have been isolated in the framework of $[\text{Ru}(\text{trpy})(\text{L})(\text{NO})]^{n+}$ [trpy = 2,2':6',2''-terpyridine, L = 2-phenylimidazo[4,5-f]1,10-phenanthroline] as the perchlorate salts $[\mathbf{4}](\text{ClO}_4)_3$ and $[\mathbf{4}](\text{ClO}_4)_2$, respectively. Single crystals of protonated material $[\mathbf{4}-\text{H}^+](\text{ClO}_4)_4 \cdot 2\text{H}_2\text{O}$ reveal a Ru–N–O bond angle of $176.1(7)^\circ$ and triply bonded N–O with a $1.127(9)$ Å bond length. Structures were also determined for precursor compounds of $[\mathbf{4}]^{3+}$ in the form of $[\text{Ru}(\text{trpy})(\text{L})(\text{Cl})](\text{ClO}_4) \cdot 4.5\text{H}_2\text{O}$ and $[\text{Ru}(\text{trpy})(\text{L}-\text{H})(\text{CH}_3\text{CN})](\text{ClO}_4)_3 \cdot \text{H}_2\text{O}$. In agreement with largely NO centered reduction, a sizable shift in $\nu(\text{NO})$ frequency was observed on moving from $[\mathbf{4}]^{3+}$ (1953 cm^{-1}) to $[\mathbf{4}]^{2+}$ (1654 cm^{-1}). The $\text{Ru}^{\text{II}}-\text{NO}^{\bullet}$ in isolated or electrogenerated $[\mathbf{4}]^{2+}$ exhibits an EPR spectrum with $g_1 = 2.020$, $g_2 = 1.995$, and $g_3 = 1.884$ in CH_3CN at 110 K, reflecting partial metal contribution to the singly occupied molecular orbital (SOMO); ^{14}N (NO) hyperfine splitting ($A_2 = 30$ G) was also observed. The plot of $\nu(\text{NO})$ versus $E^\circ(\{\text{RuNO}\}^6 \rightarrow \{\text{RuNO}\}^7)$ for 12 analogous complexes $[\text{Ru}(\text{trpy})(\text{L}')(\text{NO})]^{n+}$ exhibits a linear trend. The electrophilic $\text{Ru}-\text{NO}^+$ species $[\mathbf{4}]^{3+}$ is transformed to the corresponding $\text{Ru}-\text{NO}_2^-$ system in the presence of OH^- with $k = 2.02 \times 10^{-4}\text{ s}^{-1}$ at 303 K. In the presence of a steady flow of dioxygen gas, the $\text{Ru}^{\text{II}}-\text{NO}^{\bullet}$ state in $[\mathbf{4}]^{2+}$ oxidizes to $[\mathbf{4}]^{3+}$ through an associatively activated pathway ($\Delta S^\ddagger = -190.4\text{ J K}^{-1}\text{ M}^{-1}$) with a rate constant ($k[\text{s}^{-1}]$) of 5.33×10^{-3} . On irradiation with light (Xe lamp), the acetonitrile solution of paramagnetic $[\text{Ru}(\text{trpy})(\text{L})(\text{NO})]^{2+}$ ($[\mathbf{4}]^{2+}$) undergoes facile photorelease of NO ($k_{\text{NO}} = 2.0 \times 10^{-1}\text{ min}^{-1}$ and $t_{1/2} \approx 3.5\text{ min}$) with the concomitant formation of the solvate $[\text{Ru}^{\text{II}}(\text{trpy})(\text{L})(\text{CH}_3\text{CN})]^{2+}$ ($[\mathbf{2}]^{2+}$). The photoreleased NO can be trapped as an Mb–NO adduct.

Introduction

The research activities in the area of metal–nitrosyl chemistry have grown extensively over the recent years with the following primary perspectives: (i) understanding the bonding features of the noninnocent “NO” molecule on metalation as it can occur either as cationic NO^+ , as radical NO^{\bullet} , or as anionic NO^- , depending on the electronic nature of the ancillary ligands associated with the M–NO fragment;¹ (ii) variation of the extent of electrophilicity of the M–NO⁺ moiety and resulting reactivity profiles of M–NO⁺

with suitable nucleophiles;² (iii) mechanistic studies of the M–NO/O₂ interaction in order to understand the biological autoxidation of free NO;³ and (iv) the exploration of selective photolytic cleavage of M–NO and the eventual transfer of photoreleased “NO” to biologically relevant target molecules in order to develop alternative molecular devices capable of functioning as efficient “NO” donors under biological conditions.⁴

* To whom correspondence should be addressed. E-mail: kaim@iac.uni-stuttgart.de (W.K.), lahiri@chem.iitb.ac.in (G.K.L.).

[†] Indian Institute of Technology—Bombay.

[‡] Universität Stuttgart.

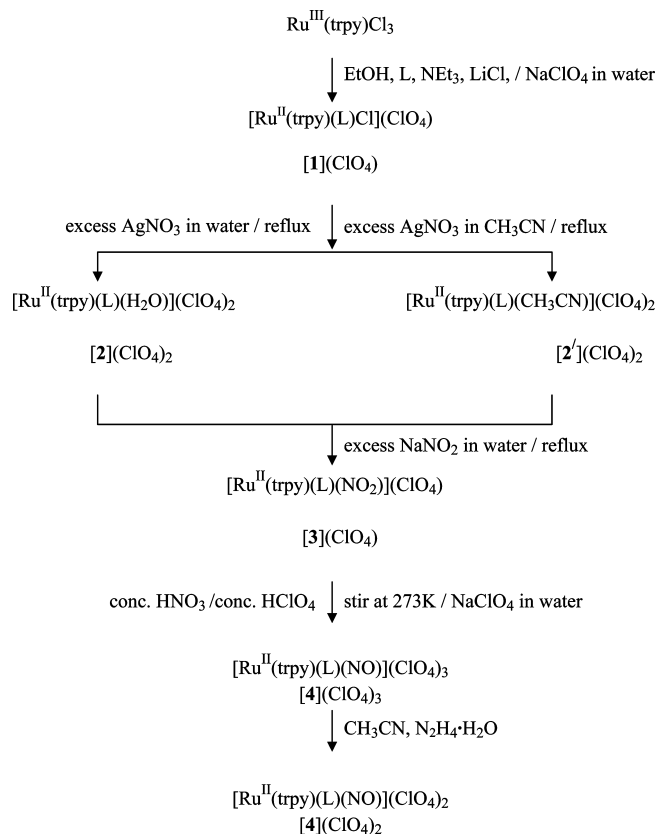
(1) (a) Videla, M.; Jacinto, J. S.; Baggio, R.; Garland, M. T.; Singh, P.; Kaim, W.; Slep, L. D.; Olabe, J. A. *Inorg. Chem.* **2006**, *45*, 8608. (b) Singh, P.; Sarkar, B.; Sieger, M.; Niemeyer, M.; Fiedler, J.; Zalis, S.; Kaim, W. *Inorg. Chem.* **2006**, *45*, 4602. (c) Sieger, M.; Sarkar, B.; Zalis, S.; Fiedler, J.; Escola, N.; Doctorovich, F.; Olabe, J. A.; Kaim, W. *Dalton Trans.* **2004**, 1797. (d) Roncaroli, F.; Baraldo, L. M.; Slep, L. D.; Olabe, J. A. *Inorg. Chem.* **2002**, *41*, 1930. (e) Slep, L. D.; Pollak, S.; Olabe, J. A. *Inorg. Chem.* **1999**, *38*, 4369.

The present work originates from the outlook of the aforesaid objectives using newly synthesized nitrosyl ruthenium derivatives $[Ru^{II}(trpy)(L)(NO^+)](ClO_4)_3 = [4](ClO_4)_3$ and $[Ru^{II}(trpy)(L)(NO^+)](ClO_4)_2 = [4'](ClO_4)_2$ ($trpy = 2,2':6',2''$ -terpyridine, $L = 2$ -phenylimidazo[4,5-*f*]1,10-phenanthroline). Although L has been of interest in the field of coordination chemistry for a number of years,⁵ only few ruthenium complexes of L and its derivatives have been reported so far from different perspectives, mainly directed at studies of interaction with DNA.⁶

Results and Discussion

Synthesis and Characterization. The nitrosyl complex $[Ru^{II}(trpy)(L)(NO)](ClO_4)_3 = [4](ClO_4)_3$ has been synthesized from the precursor $[Ru^{II}(trpy)(L)Cl](ClO_4)_4 = [1](ClO_4)_4$ via the aqua form $[Ru^{II}(trpy)(L)(H_2O)](ClO_4)_2 = [2](ClO_4)_2$ or the acetonitrile solvate $[Ru^{II}(trpy)(L)(CH_3CN)](ClO_4)_2 = [2'](ClO_4)_2$ and the nitro complex $[Ru^{II}(trpy)(L)(NO_2)](ClO_4)_4 = [3](ClO_4)_4$ (Scheme 1). Attempts of direct synthesis of pure $[4](ClO_4)_3$ either from $[1](ClO_4)_4$, $[2](ClO_4)_2$ or $[2'](ClO_4)_2$ using NO gas or $(NO)(BF_4)$ have failed, thus, the stepwise synthetic route via the nitro complex as shown in Scheme 1 was followed. The isolated nitrosyl radical species $[Ru^{II}$ -

Scheme 1



- (2) (a) Roncaroli, F.; Videla, M.; Slep, L. D.; Olabe, J. A. *Coord. Chem. Rev.* **2007**, *251*, 1903. (b) McCleverty, J. A. *Chem. Rev.* **1979**, *79*, 53. (c) Thiemens, M. H.; Trogler, W. C. *Science* **1991**, *251*, 932. (d) Feilisch, M.; Stampler, J. S., Eds. *Methods in Nitric Oxide Research*; Wiley: Chichester, England, 1996. (e) Enemark, J. H.; Feltham, R. D. *Coord. Chem. Rev.* **1974**, *13*, 339. (f) Bottomley, F. In *Reactions of Coordinated Ligands*; Braterman, P. S., Ed.; Plenum: New York, 1985; Vol. 2, p 115. (g) Bottomley, F. *Acc. Chem. Res.* **1978**, *11*, 158. (h) Ford, P. C.; Bourassa, J.; Lee, B.; Lorkovic, I.; Miranda, K.; Laverman, L. *Coord. Chem. Rev.* **1998**, *171*, 185. (i) Roncaroli, F.; Olabe, J. A. *Inorg. Chem.* **2005**, *44*, 4719. (j) Roncaroli, F.; Ruggiero, M. E.; Franco, D. W.; Estiu, G. L.; Olabe, J. A. *Inorg. Chem.* **2002**, *41*, 5760. (k) Forlano, P.; Parise, A. R.; Olabe, J. A. *Inorg. Chem.* **1998**, *37*, 6406. (l) Bottomley, F. *Coord. Chem. Rev.* **1978**, *26*, 7.
- (3) Videla, M.; Roncaroli, F.; Slep, L. D.; Olabe, J. A. *J. Am. Chem. Soc.* **2007**, *129*, 278.
- (4) (a) Halpenny, G. M.; Olmstead, M. M.; Mascharak, P. K. *Inorg. Chem.* **2007**, *46*, 6601. (b) Rose, M. J.; Olmstead, M. M.; Mascharak, P. K. *J. Am. Chem. Soc.* **2007**, *129*, 5342. (c) Rose, M. J.; Patra, A. K.; Alcid, E. A.; Olmstead, M. M.; Mascharak, P. K. *Inorg. Chem.* **2007**, *46*, 2328. (d) Patra, A. K.; Rose, M. J.; Murphy, K. A.; Olmstead, M. M.; Mascharak, P. K. *Inorg. Chem.* **2004**, *43*, 4487. (e) Videla, M.; Braslavsky, S. E.; Olabe, J. A. *Photochem. Photobiol. Sci.* **2005**, *4*, 75. (f) Zanichelli, P. G.; Miotto, A. M.; Estrela, H. F. G.; Soares, F. R.; Grassi-Kassisse, D. M.; Spadari-Bratfisch, R. C.; Castellano, E. E.; Roncaroli, F.; Parise, A. R.; Olabe, J. A.; de Brito, Alba Regina, M. S.; Franco, D. W. *J. Inorg. Biochem.* **2004**, *98*, 1921. (g) Sauer, M. G.; de Lima, R. G.; Tedesco, A. C.; da Silva, R. S. *Inorg. Chem.* **2005**, *44*, 9946. (h) Karidi, K.; Garoufis, A.; Tsipis, A.; Hadjiliadis, N.; den Dulk, H.; Reedijk, J. *Dalton Trans.* **2005**, 1176.
- (5) (a) Shavaleev, N. M.; Adams, H. A.; Weinstein, J. A. *Inorg. Chim. Acta* **2007**, *360*, 700. (b) Wei, Y.-Q.; Zhuang, B.-T.; Zhou, Z.-F.; Zhang, F. *J. Mol. Struct.* **2005**, *751*, 133.
- (6) (a) Jiang, C.-W.; Chao, H. *Polyhedron*, **2001**, *20*, 2187. (b) Xiong, Y.; He, X.-F.; Zou, X.-H.; Wu, J.-Z.; Chen, X.-M.; Ji, L.-N.; Li, R.-H.; Zhou, J.-Y.; Yu, K.-B. *J. Chem. Soc., Dalton Trans.* **1999**, 19. (c) Wu, J.-Z.; Ye, B.-H.; Wang, L.; Ji, L.-N.; Zhou, J.-Y.; Li, R.-H.; Zhou, Z.-Y. *J. Chem. Soc., Dalton Trans.* **1997**, 1395. (d) Wu, J.-Z.; Li, L.; Zeng, T.-X.; Ji, L.-N.; Zhou, J.-Y.; Luo, T.; Li, R.-H. *Polyhedron* **1997**, *16*, 103. (e) Uma Maheswari, P.; Palaniandavar, M. *J. Inorg. Biochem.* **2004**, *98*, 219. (f) Jiang, C.-W.; Chao, H.; Li, R.-H.; Li, H.; Ji, L.-N. *J. Coord. Chem.* **2003**, *56*, 147. (g) Chao, H.; Li, R.-H.; Jiang, C.-W.; Li, H.; Ji, L.-N.; Li, X.-Y. *J. Chem. Soc., Dalton Trans.* **2001**, 1920. (h) Zheng, K. C.; Deng, H.; Liu, X. W.; Li, H.; Chao, H.; Ji, L. N. *J. Mol. Struct.* **2004**, *682*, 225. (i) Li, J.; Xu, L.-C.; Chen, J.-C.; Zheng, K. C.; Ji, L.-N. *J. Phys. Chem. A* **2006**, *110*, 8174. (j) Tan, L.-F.; Chao, H.; Zhou, Y.-F.; Ji, L.-N. *Polyhedron* **2007**, *26*, 3029.

($trpy)(L)(NO^+)$)($ClO_4)_2 = [4'](ClO_4)_2$ has been prepared by reducing $[4](ClO_4)_3$ chemically using hydrazine hydrate. Electrochemical reduction of $[4]^{3+}$ leads to the quantitative formation of $[4]^{2+}$ which can then be reversibly oxidized to $[4]^{3+}$.

The diamagnetic compounds $[1](ClO_4)_4$, $[2](ClO_4)_2$, $[2'](ClO_4)_2$, $[3](ClO_4)_4$, and $[4](ClO_4)_3$ and the doublet species $[4](ClO_4)_2$ exhibit 1:1, 1:2, 1:2, 1:1, 1:3, and 1:2 conductivities, respectively, and give satisfactory microanalytical data (see the Experimental Section). The electrospray mass spectra of $[1](ClO_4)_4$, $[2](ClO_4)_2$, $[2'](ClO_4)_2$, $[3](ClO_4)_4$, $[4](ClO_4)_3$, and $[4](ClO_4)_2$ in CH_3CN show molecular ion peaks centered at $m/z = 665.94$, 730.05 , 729.93 , 677.08 , 730.72 , and 730.42 , respectively, corresponding to $\{[1](ClO_4) - ClO_4\}^+$ (calculated molecular mass: 666.07), $\{[2](ClO_4)_2 - ClO_4 - H_2O\}^+$ (calculated molecular mass: 730.05), $\{[2'](ClO_4)_2 - ClO_4 - CH_3CN\}^+$ (calculated molecular mass: 730.05), $\{[3](ClO_4)_4 - ClO_4\}^+$ (calculated molecular mass: 677.09), $\{[4](ClO_4)_3 - 2ClO_4 - NO\}^+$ (calculated molecular mass: 730.05), and $\{[4](ClO_4)_2 - ClO_4 - NO\}^+$ (calculated molecular mass: 730.05), respectively (Figure 1).

The molecular structures of the cationic, partially protonated complexes in crystals of $[1](ClO_4)_4 \cdot 4.5H_2O$, $[2'-H^+](ClO_4)_3 \cdot H_2O$ and $[4-H^+](ClO_4)_4 \cdot 2H_2O$ are shown in Figures 2–4. Crystallographic parameters and selected bond distances and angles are listed in Tables S1 and S2 (see the Supporting Information). In spite of numerous attempts, the quality of the crystals remained low; however, the bond distances and angles match reasonably with similar complexes reported earlier.⁷ The lattice of $[1](ClO_4)_4 \cdot 4.5H_2O$

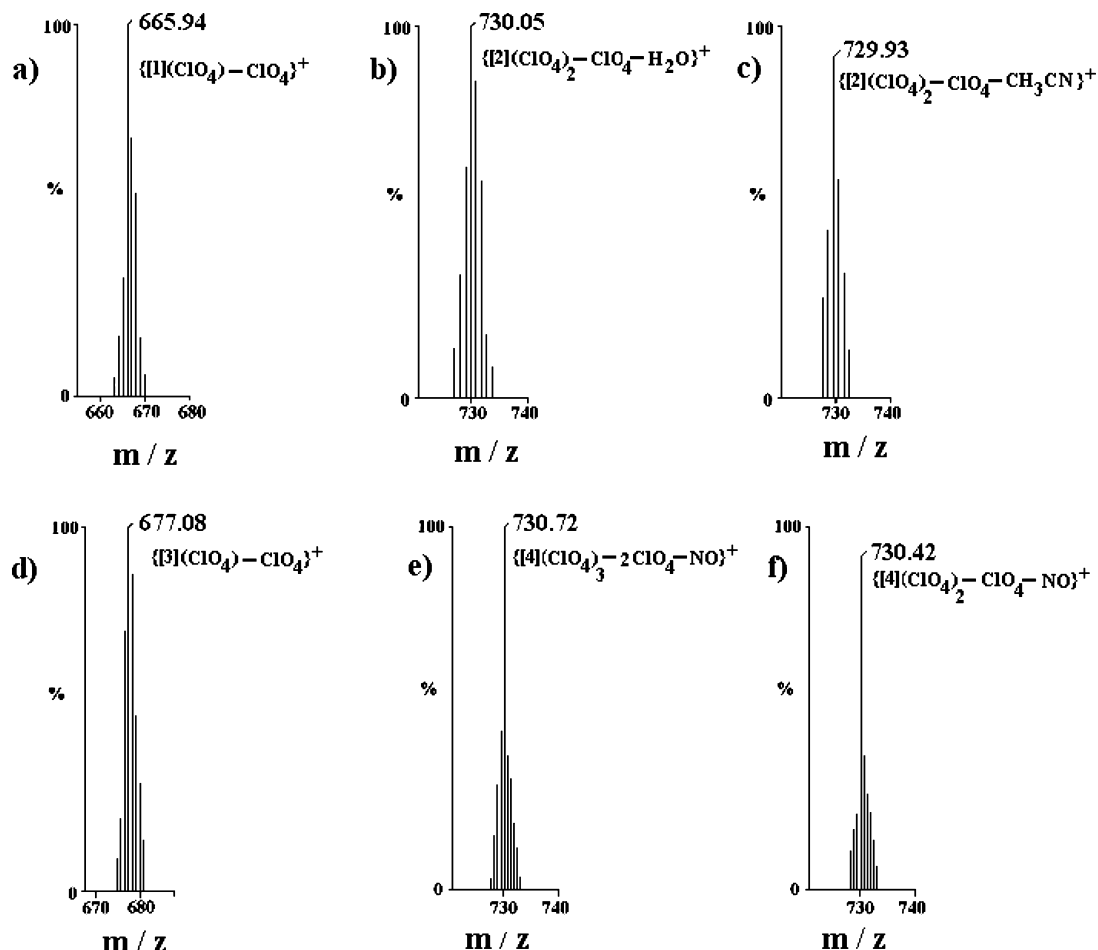


Figure 1. ESI mass spectra of (a) $[1](\text{ClO}_4)$, (b) $[2](\text{ClO}_4)_2$, (c) $[2'](\text{ClO}_4)_2$, (d) $[3](\text{ClO}_4)$, (e) $[4](\text{ClO}_4)_3$, and (f) $[4](\text{ClO}_4)_2$ in CH_3CN .

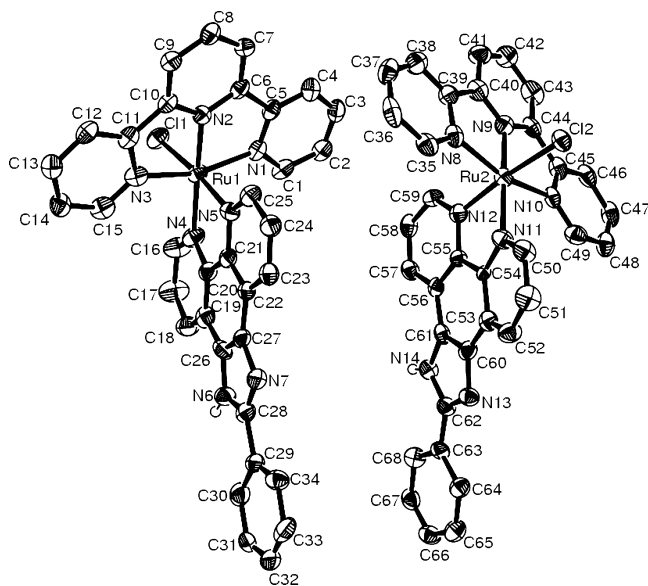


Figure 2. Molecular structure of the nonequivalent cations $[\text{Ru}(\text{trpy})(\text{L})(\text{Cl})]^+$ in the asymmetric unit of the crystal of $[1](\text{ClO}_4) \cdot 4.5\text{H}_2\text{O}$.

consists of two crystallographically independent molecules (Figure 2) which differ conspicuously in the relative orientation of the imidazole of L and the Ru–Cl bond. The acetonitrile complex has become protonated at the basic imine N of the imidazole ring to $[\text{Ru}^{\text{II}}(\text{trpy})(\text{L}-\text{H}^+)(\text{CH}_3\text{CN})](\text{ClO}_4)_3$ during the crystallization process from a CH_3CN –benzene (1:1)

mixture over a period of 1 month (Figure 3). The linearity of the Ru^{II}–N(8)–O(1) bond ($176.1(7)^\circ$) and the triple bond feature of N(8)–O(1) ($1.127(9) \text{ \AA}$) support the electrophilic NO⁺ character in $[\text{Ru}^{\text{II}}(\text{trpy})(\text{L}-\text{H}^+)(\text{NO})](\text{ClO}_4)_4 \cdot 2\text{H}_2\text{O}$; additional evidence from the ν_{NO} stretching frequency and $E^\circ(\text{Ru}^{\text{II}}-\text{NO}^+/\text{Ru}^{\text{II}}-\text{NO}^*)$ will be described later.⁷ In all cases, the ligand L forms a five-membered chelate ring with the metal ion via the nitrogen donor centers of the phenanthroline unit.^{6b}

Spectral Aspects. The ¹H NMR spectra of diamagnetic $[1](\text{ClO}_4)$, $[2](\text{ClO}_4)_2$, $[2'](\text{ClO}_4)_2$, $[3](\text{ClO}_4)$, and $[4](\text{ClO}_4)_3$ in $(\text{CD}_3)_2\text{SO}$ (Figure S1, Supporting Information, and Experimental Section) display severe overlap of the expected 22 signals in the aromatic region between 7.0 and 10.5 ppm, 11 resonances each from the trpy and the L ligand. The chemical shift of the resonances varies slightly depending on the monodentate ligands, Cl[−], H₂O, CH₃CN, NO₂[−], or NO⁺. The N–H proton of the imidazole ring of coordinated L has only been observed for $[1](\text{ClO}_4)$ at 14.4 ppm.⁸ The absence of the N–H signal of the coordinated L in the other complexes can be attributed to rapid exchange.^{6j} The signal due to the CH₃ group of coordinated acetonitrile in $[2'](\text{ClO}_4)_2$ appears at 2.38 ppm. While single crystals for X-ray diffraction were obtained in an imidazole-protonated form for the complexes with the electrophilic CH₃CN and NO⁺ monodentate ligands (see above), the dissolved species are identified as the imidazole forms with neutral L

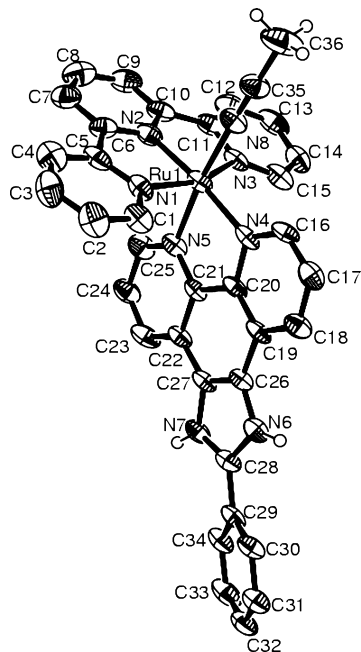


Figure 3. Molecular structure of the trication $[Ru(trpy)(L-H^+)(CH_3CN)]^{3+}$ in the crystal of $[2'-H^+](ClO_4)_3 \cdot 2H_2O$.

according to elemental analysis, molar conductivity, and 1H NMR data.

The $\nu(ClO_4^-)$ vibrations are observed at 1096/623, 1089/625, 1088/625, 1097/623, 1087/626, and 1091/628 cm^{-1} for $[1](ClO_4)$, $[2](ClO_4)_2$, $[2'](ClO_4)_2$, $[3](ClO_4)$, $[4](ClO_4)_3$, and $[4](ClO_4)_2$, respectively. The typical $Ru-NO_2$ frequencies of $[3](ClO_4)$ appear at 1338 cm^{-1} (asymmetric) and 1272 cm^{-1} (symmetric). The ν_{NO} stretching frequency of $[4](ClO_4)_3$ at 1948 cm^{-1} is lower than that reported for analogous complexes $\{Ru^II(trpy)(L')(NO^+)\}$ with $L' =$ strongly π -acidic $L^3 = 1952$ cm^{-1} , $L^2 = 1957$ cm^{-1} , $L^1 = 1960$ cm^{-1} (Table 1). However, it is much higher than that observed with strongly σ -donating $L^{10} = 1858$ cm^{-1} and $L^9 = 1914$ cm^{-1} and close to that found for moderately π -acidic $L^5 = 1949$ cm^{-1} (Table 1). The observed ν_{NO} value of $[4](ClO_4)_3$ is thus suggestive of a moderately strong electrophilic character of NO. On reduction of $[4]^{3+}$ to $[4]^{2+}$ the ν_{NO} frequency is substantially reduced from 1948 (solid)/1953 (acetonitrile solution) cm^{-1} to 1634 (solid)/1654 (acetonitrile solution) cm^{-1} (Figure 5). The large shift in ν_{NO} frequency, $\Delta\nu = 314$ (solid)/300(solution) cm^{-1} , on moving from $[4]^{3+}$ to $[4]^{2+}$ agrees with a transformation of linear $Ru^{II}-NO^+$, $\{RuNO\}$,⁶ to most likely bent $Ru^{II}-NO^*$, $\{RuNO\}$.^{7,1c,2b,9}

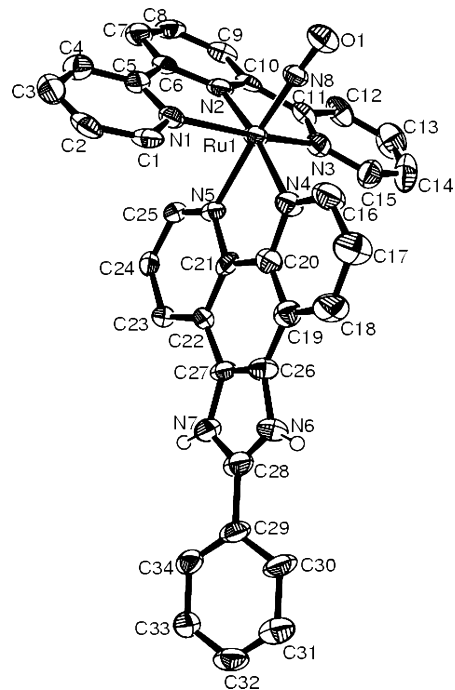


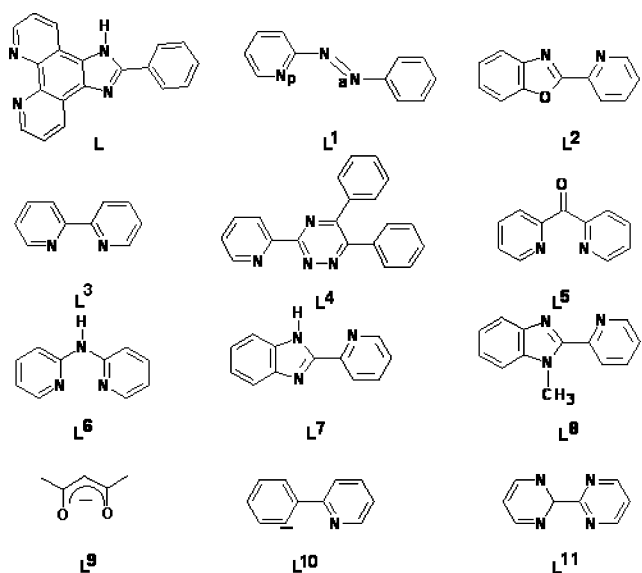
Figure 4. Molecular structure of the tetracation $[Ru(trpy)(L-H^+)(NO)]^{4+}$ in the crystal of $[4-H^+](ClO_4)_4 \cdot 2H_2O$.

The complexes exhibit ruthenium(II) based metal to ligand charge transfer (MLCT) transitions to $\pi^*(trpy)$ and $\pi^*(L)$ orbitals near 500 nm and ligand based multiple transitions in the UV region (Figure 6, Table 2). The MLCT band energy in acetonitrile solution follows the order $[1]^+ (509 \text{ nm}) < [4]^{2+} (486 \text{ nm}) < [3]^+ (478 \text{ nm}) < [2]^{2+} (462 \text{ nm}) \approx [2']^{2+} (461 \text{ nm}) < [4]^{3+} (370 \text{ nm})$, depending on the relative stabilization of the $d\pi(Ru)$ level.⁷ The high energy shift of the MLCT band in $[4]^{3+}$ implies a strong $d\pi(Ru^{II}) \rightarrow \pi^*(NO^+)$ back-bonding interaction. This has further been evidenced in the observed short $Ru-N8(NO)$ bond distance of 1.766(7) Å (Table S2) and the relatively high ν_{NO} frequency of 1948 cm^{-1} . Electronic spectra of $[2]^{2+}$ in solvents of different polarity show moderate variation (Table 2, Figure 6).¹⁰

The complexes are found to be luminescent in frozen solution, the nitro derivative $[3]^+$ displaying the strongest emission. The excitation of $[1]^+$, $[2]^{2+}$, $[2']^{2+}$, $[3]^+$, or $[4]^{3+}$ at the respective MLCT bands in EtOH:MeOH (4:1) glass at 77 K shows emission at $\lambda_{emis} = 705 \text{ nm}$ ($\Phi = 0.022$) (Φ corresponds to the quantum yield at 77 K with reference to $[Ru(bpy)_3](PF_6)_2$, $\Phi = 0.34^{11}$), 675 nm ($\Phi = 0.038$), 597 nm ($\Phi = 0.025$), 623 nm ($\Phi = 0.20$), and 580 nm ($\Phi = 0.11$), respectively (Figure 6). The observed emissions are thought to

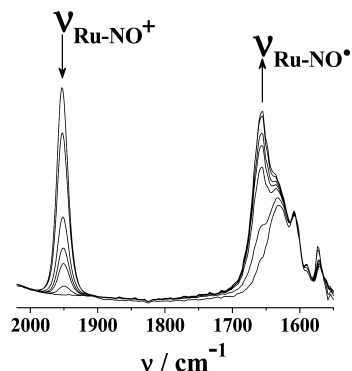
(7) (a) Mondal, B.; Paul, H.; Puranik, V. G.; Lahiri, G. K. *J. Chem. Soc., Dalton Trans.* **2001**, 481. (b) Chanda, N.; Paul, D.; Kar, S.; Mobin, S. M.; Datta, A.; Puranik, V. G.; Rao, K. K.; Lahiri, G. K. *Inorg. Chem.* **2005**, *44*, 3499. (c) Pipes, D. W.; Meyer, T. J. *Inorg. Chem.* **1984**, *23*, 2466. (d) Maji, S.; Chatterjee, C.; Mobin, S. M.; Lahiri, G. K. *Eur. J. Inorg. Chem.* **2007**, 3425. (e) Sarkar, S.; Sarkar, B.; Chanda, N.; Kar, S.; Mobin, S. M.; Feidler, J.; Kaim, W.; Lahiri, G. K. *Inorg. Chem.* **2005**, *44*, 6092. (f) Chanda, N.; Mobin, S. M.; Puranik, V. G.; Datta, A.; Niemeyer, M.; Lahiri, G. K. *Inorg. Chem.* **2004**, *43*, 1056. (g) Dovelotoglou, A.; Adeyemi, S. A.; Meyer, T. J. *Inorg. Chem.* **1996**, *35*, 4120. (h) Hadadzadeh, H.; DeRosa, M. C.; Yap, G. P. A.; Rezvani, A. R.; Crutchley, R. J. *Inorg. Chem.* **2002**, *41*, 6521. (i) Singh, P.; Fiedler, J.; Zális, S.; Duboc, C.; Niemeyer, M.; Lissner, F.; Schleid, T.; Kaim, W. *Inorg. Chem.* **2007**, *46*, 9254.

(8) (a) Maji, S.; Patra, S.; Chakraborty, S.; Mobin, S. M.; Janardanan, D.; Sunoj, R. B.; Lahiri, G. K. *Eur. J. Inorg. Chem.* **2007**, 314. (b) Chakraborty, S.; Walawalkar, M. G.; Lahiri, G. K. *J. Chem. Soc., Dalton Trans.* **2000**, 2875. (c) Hirsch-Kuchma, M.; Nicholson, T.; Davison, A.; Davis, W. M.; Jones, A. G. *Inorg. Chem.* **1997**, *36*, 3237. (9) (a) Wanner, M.; Scheiring, T.; Kaim, W.; Slep, L. D.; Baraldo, L. M.; Olabe, J. A.; Zalis, S.; Baerends, E. *J. Inorg. Chem.* **2001**, *40*, 5704. (b) Haymore, B. L.; Ibers, J. A. *Inorg. Chem.* **1975**, *14*, 3060. (c) Gaughan, A. P.; Haymore, B. L.; Ibers, J. A.; Myers, W. H.; Nappier, T. F.; Meeck, D. W. *J. Am. Chem. Soc.* **1973**, *95*, 6859. (d) Pandey, K. K. *Coord. Chem. Rev.* **1992**, *121*, 1. (10) Mondal, B.; Walawalkar, M. G.; Lahiri, G. K. *J. Chem. Soc., Dalton Trans.* **2000**, 4209.

Table 1. Reduction Potentials of the {Ru(NO⁺)} → {Ru(NO[•])} Process and ν_{NO} Values for {Ru^{II}(trpy)(L')(NO)}³⁺

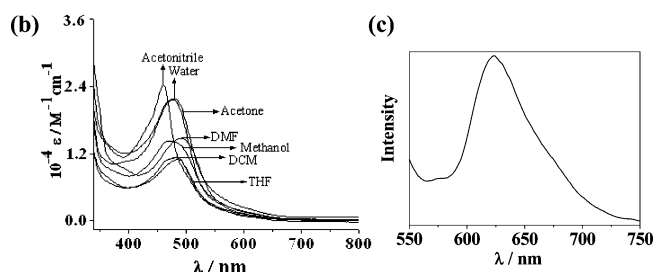
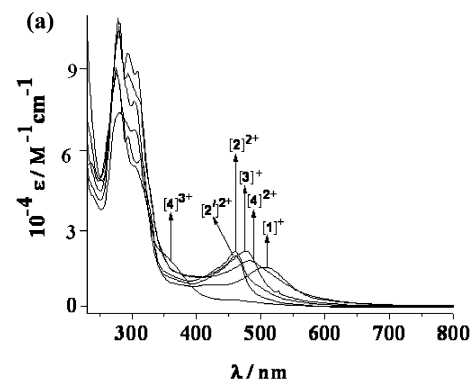
L'	E_{298}° [V] ^a	$\nu(\text{NO})$ (cm ⁻¹) ^b	refs
L ¹	0.72	1960	7a
L	0.49	1948	present work
L ²	0.45	1957	7b
L ³	0.45	1952	7c
L ⁴	0.40	1944	7d
L ⁵	0.36	1949	7e
L ⁶	0.34	1945	7f
L ⁷	0.33	1940	7b
L ⁸	0.31	1932	7b
L ⁹	0.02	1914	7g
L ¹⁰	-0.28	1858	7h
L ¹¹	0.40	1957	7i

^a CH₃CN/0.1 M Et₄NClO₄/SCE. ^b In KBr disk.

**Figure 5.** IR spectral changes for the conversion [4]³⁺ → [4]²⁺ from optically transparent thin layer electrode (OTTLE) spectroelectrochemistry in CH₃CN/0.1 M Bu₄NPF₆ with stepwise variation of the potential. Bands below 1650 cm⁻¹ arise from ring vibrations.

originate from the triplet (³MLCT) excited states as observed in numerous ruthenium–polypyridine complexes.¹²

Redox Properties. The Ru^{III}/Ru^{II} potentials of [1]⁺, [2']²⁺, and [3]⁺ in CH₃CN and of [2]²⁺ in H₂O (Table 3) vary in the order of Cl⁻ < H₂O < NO₂⁻ < CH₃CN for the monodentate ligand.⁷ The presence of Ru^{III} in the

**Figure 6.** (a) Electronic spectra in acetonitrile of [1]⁺, [2]²⁺, [2']²⁺, [3]⁺, [4]³⁺, and [4]²⁺. (b) Electronic spectra of [2]²⁺ in different solvents. (c) Emission spectrum of [3](ClO₄) in 4:1 EtOH–MeOH at 77 K.**Table 2.** Electronic Spectral Data of Complexes

compound	solvent	λ [nm] (ϵ [M ⁻¹ cm ⁻¹])
[1](ClO ₄)	acetonitrile	509(18611), 314(56016), 294(59038), 276(82142), 236(53332)
[2](ClO ₄) ₂	acetonitrile	462(25718), 303(71232), 293(75163), 282(97862), 276(100079), 222(60149)
	methanol	479(13587), 310(57673), 277(81613), 203(69519)
	water	477(22789), 310(90825), 222(82525), 310(90825)
	acetone	477(22949), 323(53235), 312(18958), 272(16284)
	tetrahydrofuran	481(11975), 312(46252), 292(50562), 281(58223), 235(33107)
	dichloromethane	485(11975), 310(49245), 294(52556), 280(65885), 225(39588)
	dimethylformamide	497(15606), 316(66204), 296(70873), 281(69875), 246(23627), 236(36276)
[2'](ClO ₄) ₂	acetonitrile	461(24924), 305(60845), 292(64340), 281(67292), 244(37325), 221(55015)
[3](ClO ₄)	acetonitrile	478(26062), 308(94246), 293(93837), 279(100509), 220(74543)
[4](ClO ₄) ₃	acetonitrile	370(17921), 305(52234), 279(63725), 276(67140), 222(55998)
[4](ClO ₄) ₂	acetonitrile	488(22696), 329(51801), 313(95981), 303(102867), 293(108636), 278(128496)

oxidized solutions has been established only for the complex [2']³⁺ via its typical rhombic EPR spectrum ($g_1 = 2.444$, $g_2 = 2.201$, $g_3 = 1.851$; Figure S2 in the Supporting Information). The potentials are in general comparable to those of the analogous [Ru^{II}(trpy)(L')(X)]ⁿ⁺ complexes (X = Cl⁻, NO₂⁻, H₂O, or CH₃CN) and vary

(11) (a) Alsasser, R.; Van Eldik, R. *Inorg. Chem.* **1996**, *35*, 628. (b) Chen, P.; Duesing, R.; Graff, D. K.; Meyer, T. J. *J. Phys. Chem.* **1991**, *95*, 5850.

(12) (a) Kar, S.; Chanda, N.; Mobin, S. M.; Datta, A.; Urbanos, F. A.; Puranik, V. G.; Jimenez-Aparicio, R.; Lahiri, G. K. *Inorg. Chem.* **2004**, *43*, 4911. (b) Sarkar, B.; Laye, R. H.; Mondal, B.; Chakraborty, S.; Paul, R. L.; Jeffery, J. C.; Puranik, V. G.; Ward, M. D.; Lahiri, G. K. *J. Chem. Soc., Dalton Trans.* **2002**, 2097. (c) Juris, A.; Balzani, V.; Barigelletti, F.; Campagna, S.; Belser, P.; von Zelewsky, A. *Coord. Chem. Rev.* **1988**, *84*, 85.

Table 3. Redox Potentials of Complexes^{a,b}

compound	Ru ^{III} /Ru ^{II}	couple		trpy reduction	
		NO ⁺ → NO [*]	NO [*] → NO ⁻		
[1](ClO ₄)	0.69(66)			-1.53(54)	-1.80(60)
[2](ClO ₄) ₂ ^c	0.84(84)			-1.59(53)	-1.93(67)
[2'](ClO ₄) ₂	1.22(95)			-1.58(66)	-1.99(62)
[3](ClO ₄)	1.03(90)			-1.44(94)	-1.97(58)
[4](ClO ₄) ₃		0.49(110)	-0.26(154) ^d	-1.17(72)	-1.43(51)

^a Potentials E_{298° [V] (ΔE [mV]) versus SCE. ^b In CH₃CN/0.1 M Et₄NClO₄. ^c In H₂O/0.1 M NaClO₄. ^d Quasi-reversible.

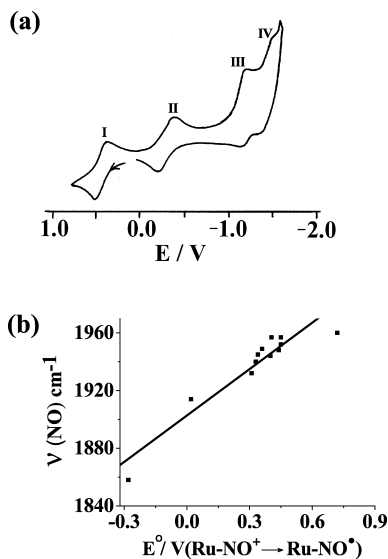


Figure 7. (a) Cyclic voltammogram of [4](ClO₄)₃ in CH₃CN/0.1 M Et₄NClO₄. (b) Least-squares plot of E° [V] { $[Ru(NO^+)/Ru(NO^*)]$ } versus $\nu(NO)/cm^{-1}$ of twelve related complexes as listed in Table 1; $\nu(NO)$ [cm^{-1}] = $1903\text{ cm}^{-1} + 107\text{ cm}^{-1}/VE^\circ$ [V], $R = 0.943$.

according to the electronic aspects of L' .⁷ The trpy ligand-based reductions are observed in the range between -1.44 and -1.99 V (Table 3).¹³

The nitrosyl based reductions involving the $NO^+ \rightarrow NO^*$ and $NO^* \rightarrow NO^-$ conversion in $[4]^{n+}$ appear at +0.49 and -0.26 V versus standard calomel electrode (SCE) (couples I and II, Figure 7a, Table 3).⁷ The tricationic charge of $[4]^{3+}$ facilitates the reversible reduction of the coordinated NO^+ to NO^* to occur at a rather high potential, and that effect is even extended to the second one-electron reduction ($NO^* \rightarrow NO^-$). The 0.75 V potential difference between the successive NO centered reductions (couples I and II) gives rise to a comproportionation constant (K_c) of $10^{12.7}$ ($RT \ln K_c = \Delta E/0.059$ (see ref 14) where $\Delta E = 0.75$ V) for the intermediate (radical) species $[4]^{2+}$. This large K_c value reflects the chemical stability of the intermediate which facilitated its isolation in the solid state. The EPR spectrum of $[4]^{2+}$ exhibits g components at $g_1 = 2.020$, $g_2 = 1.995$,

- (13) (a) Mondal, B.; Puranik, V. G.; Lahiri, G. K. *Inorg. Chem.* **2002**, *41*, 5831. (b) Chanda, N.; Mondal, B.; Puranik, V. G.; Lahiri, G. K. *Polyhedron* **2002**, *21*, 2033. (c) Catalano, V. J.; Heck, R. A.; Ohman, A.; Hill, M. G. *Polyhedron* **2000**, *19*, 1049. (d) Catalano, V. J.; Heck, R. A.; Immoos, C. E.; Ohman, A.; Hill, M. G. *Inorg. Chem.* **1998**, *37*, 2150. (e) Patra, S.; Sarkar, B.; Ghuman, S.; Patil, M. P.; Mobin, S. M.; Sunoj, R. B.; Kaim, W.; Lahiri, G. K. *Dalton Trans.* **2005**, 1188. (f) Hedda, T. B.; Bozec, H. L. *Inorg. Chim. Acta* **1993**, *204*, 103. (g) Deacon, G. B.; Patrick, J. M.; Skelton, B. W.; Thomas, N. C.; White, A. H. *Aust. J. Chem.* **1984**, *37*, 929.
- (14) Creutz, C. *Prog. Inorg. Chem.* **1983**, *30*, 1.

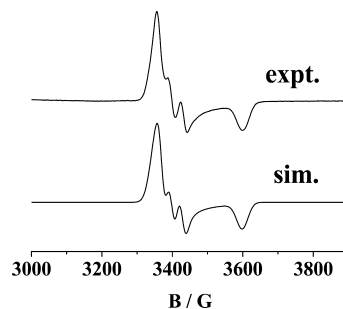
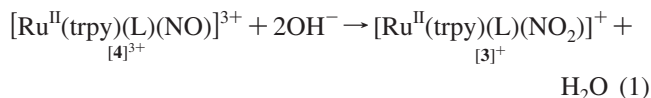


Figure 8. Experimental (top) and computer simulated (bottom) EPR spectrum at 110 K of the radical complex $[4]^{2+}$ generated by reduction of $[4](ClO_4)_3$ in CH₃CN/0.1 M Bu₄NPF₆.

and $g_3 = 1.884$ with an NO hyperfine splitting $A_2(^{14}N)$ of 30 G in CH₃CN at 110 K (Figure 8). The pronounced anisotropic profile of the spectrum arises from close lying $\pi^*(NO)$ orbitals ($g_{av} < 2$) and from the partial contribution of the metal ion to the singly occupied molecular orbital (SOMO).^{1c,2b,9a,15} The similarity of the EPR parameters with those observed and interpreted previously^{9a,15a} is compatible with contributions of about $1/3$ from the metal ion and $2/3$ from the NO group to the SOMO, implying a mixed resonance formulation $\{Ru^I(NO^+)\} \leftrightarrow \{Ru^II(NO^*)\}$.^{9a} The stepwise reduction of coordinated trpy is observed at -1.17 and -1.43 V (couples III and IV, Figure 7a, Table 3). The $Ru^{II}-NO^+ \rightarrow Ru^{II}-NO^*$ reduction potentials for analogous complexes with different ligands L' (L^1-L^{11} , L) and the corresponding $\nu(NO)$ values (Table 1) follow a linear trend (Figure 7b).⁷

Reaction of $[Ru^{II}(trpy)(L)(NO^+)]^{3+}$ ($[4]^{3+}$) with OH^- . In spite of the relatively high $\nu(NO)$ stretching frequency of 1948 cm^{-1} for $[4]^{3+}$, suggesting facile nucleophilic attack, this complex ion is found to be persistent both in the solid and in CH₃CN solution; it is only sparingly soluble in water. However, it undergoes facile transformation to the corresponding nitro derivative $[3]^+$ under alkaline conditions in CH₃CN. Due to the poor solubility of $[4]^{3+}$ and the virtually insoluble nature of the nitro derivative $[3]^+$ in water (cf. its preparation) the conversion had to be performed in CH₃CN. The conversion process (eq 1)



was monitored spectrophotometrically in the temperature range 303–323 K in CH₃CN in the presence of aqueous NaOH solution ($[4]^{3+}$, 0.22×10^{-4} M, and NaOH, 0.2×10^{-2} M; pseudo pH ~ 10). The well-defined isobestic points (Figure 9) are indicative of a clean conversion (1). The pseudo-first-order rate constants (k [s^{-1}]) at three different temperatures are: 2.02×10^{-4} (303 K), 3.97×10^{-4} (313 K), 6.37×10^{-4} (323 K). The activation parameters ($\Delta H^\ddagger/$

- (15) (a) Frantz, S.; Sarkar, B.; Sieger, M.; Kaim, W.; Roncaroli, F.; Olabe, J. A.; Zalis, S. *Eur. J. Inorg. Chem.* **2004**, *14*, 2902. (b) de Souza, V. R.; da Costa Ferreira, A. M.; Toma, H. E. *Dalton Trans.* **2003**, 458. (c) McGarvey, B. R.; Ferro, A. A.; Tfouni, E.; Bezerra, C. W. D.; Bagatin, I. A.; Franco, D. W. *Inorg. Chem.* **2000**, *39*, 3577. (d) Callahan, R. W.; Meyer, T. J. *Inorg. Chem.* **1977**, *16*, 574. (e) Diversi, P.; Fontani, M.; Fuligni, M.; Laschi, F.; Marchetti, F.; Matteoni, S.; Pinzino, C.; Zanello, P. *J. Organomet. Chem.* **2003**, *675*, 21.

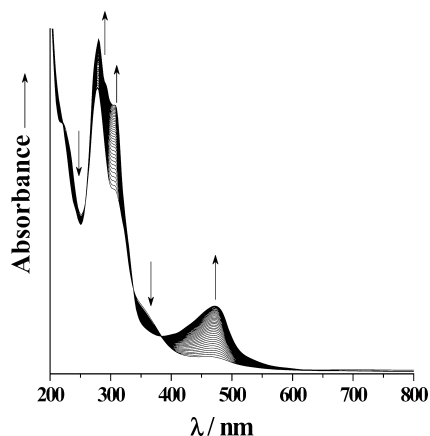


Figure 9. Time evolution of the electronic spectrum (5 min time intervals) of a solution of $[\text{Ru}(\text{trpy})(\text{L})(\text{NO})]^{3+}$ ($[\mathbf{4}]^{3+}$, 0.22×10^{-4} M) in the presence of OH^- (0.2×10^{-2} M; pseudo pH ~ 10) in CH_3CN at 313 K.

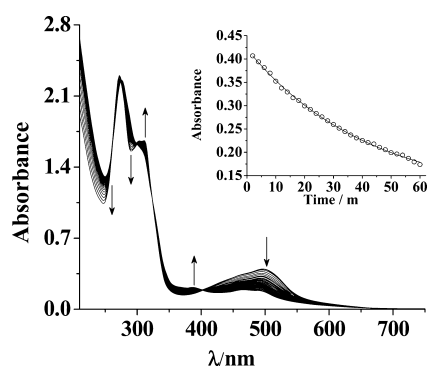


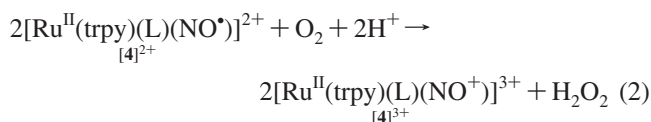
Figure 10. (a) Time evolution of the electronic spectrum (2 min time intervals) of a solution of $[\text{Ru}(\text{trpy})(\text{L})(\text{NO})]^{2+}$ ($[\mathbf{4}]^{2+}$, 0.12×10^{-4} M) in $\text{CH}_3\text{CN}/0.1$ M HClO_4 under a steady flow of O_2 . The inset shows a steady decrease of 488 nm absorption corresponding to $[\mathbf{4}]^{2+}$.

ΔS^\ddagger) and equilibrium constant (K) values are calculated as 44.24 $\text{kJ M}^{-1}/-169.54$ $\text{J K}^{-1} \text{M}^{-1}$, and 88, respectively. The large negative ΔS^\ddagger value implies that the nucleophilic attack of OH^- to the electrophilic NO^+ center in $[\mathbf{4}]^{3+}$ takes place through an associatively activated process.⁷ The equilibrium constant of 88 suggests that the nitro species $[\text{Ru}^{\text{II}}(\text{trpy})(\text{L})(\text{NO}_2)]^+$ ($[\mathbf{3}]^+$) exists as the main component.

The slope of the plot of pseudo-first-order rate constant values (k [s^{-1}]), 2.02×10^{-4} , 3.88×10^{-4} , 9.97×10^{-4} in CH_3CN ($[\mathbf{4}]^{3+}$, 0.22×10^{-4} M) at three different concentrations of OH^- of 0.2×10^{-2} , 0.4×10^{-2} , and 1.0×10^{-2} M, respectively, yields the second order rate constant value of $9.9 \times 10^{-2} \text{M}^{-1} \text{s}^{-1}$. The estimated low rate constant value of $9.9 \times 10^{-2} \text{M}^{-1} \text{s}^{-1}$ for reaction 1 in CH_3CN as compared to the second-order rate constant (k [$\text{M}^{-1} \text{s}^{-1}$]) values obtained for the analogous reported complexes $[\text{Ru}^{\text{II}}(\text{trpy})(\text{L})(\text{NO})]^{3+}$ (Table 1) in H_2O L¹, 6.94×10^5 ; L², 4.7×10^3 ; L⁵, 2.46×10^3 ; L⁶, 1.7×10^3 ; L⁸, 1.1×10^3 (assuming that the concentration of OH^- in H_2O medium is 10^{-7} M) can be considered primarily due to the effect of the nonaqueous CH_3CN medium. A similar effect of the nonaqueous CH_3CN solvent on the rate constant value of reaction 1 has also been observed in the case of $[\text{Ru}^{\text{II}}(\text{trpy})(\text{L}^4)(\text{NO})]^{3+}$ (k , $0.4 \times 10^{-2} \text{M}^{-1} \text{s}^{-1}$).^{7d}

Reaction of $[\text{Ru}^{\text{II}}(\text{trpy})(\text{L})(\text{NO})]^{2+}$ ($[\mathbf{4}]^{2+}$) with O_2 . The reaction of dioxygen with the metal bound nitrosyl group

$\{\text{MNO}\}^7$ has been studied since long in the light of understanding the biological NO autoxidation process.³ Mechanistic studies with a variety of transition metal–NO species suggest the formation of nitrate or nitrito complexes which proceeds via the intermediacy of an O-bound or N-bound peroxyxynitrite complex.¹⁶ Therefore, the reaction of O_2 with the nitrosyl species $[\text{Ru}^{\text{II}}(\text{trpy})(\text{L})(\text{NO}^*)]^{2+}$ ($[\mathbf{4}]^{2+}$) was followed spectrophotometrically at three different temperatures (298, 308, 318 K) in acetonitrile in the presence of 0.1 M HClO_4 (acetonitrile was used due to the poor solubility of $[\mathbf{4}]^{2+}$ in water). Though $[\mathbf{4}]^{2+}$ is stable in acetonitrile under atmospheric conditions, in the presence of a steady flow of dioxygen gas it slowly transforms to the corresponding NO^+ species $[\mathbf{4}]^{3+}$ (Figure 10) which can be represented by eq 2.^{1a}



The isosbestic points in Figure 10 reveal the exclusive involvement of two primary components ($[\mathbf{4}]^{2+}/[\mathbf{4}]^{3+}$) during the transformation process at the spectrophotometric time scale. The pseudo first order rate constants (k [s^{-1}]) at three different temperatures are the following: 5.33×10^{-3} (298 K), 7.82×10^{-3} (308 K), and 11.96×10^{-3} (318 K). The activation parameters ΔH^\ddagger and ΔS^\ddagger are calculated as $+29.3$ kJ M^{-1} and -190.4 $\text{J K}^{-1} \text{M}^{-1}$, respectively. On the basis of the thermodynamic parameters, particularly the large negative ΔS^\ddagger value, it may be proposed that the reaction proceeds through an associatively activated pathway involving the initial binding of O_2 with the M–NO fragment. The same reaction (eq 2) has also been tested using air instead of oxygen gas under similar experimental conditions at 298 K, and the estimated pseudo-first-order rate constant value is found to be decreased significantly to $2.416 \times 10^{-3} \text{s}^{-1}$.

Photocleavage of the Ru^{II} –NO Bond in $[\text{Ru}^{\text{II}}(\text{trpy})(\text{L})(\text{NO}^*)]^{2+}$ ($[\mathbf{4}]^{2+}$) and Binding of Photoreleased NO with Myoglobin (Mb). The nitrosyl complex $[\text{Ru}^{\text{II}}(\text{trpy})(\text{L})(\text{NO}^+)]^{3+}$ ($[\mathbf{4}]^{3+}$) was found to be stable in acetonitrile solution under ambient light conditions as well as under irradiation with a Xenon 350 W lamp. However, on exposure to such light the deoxygenated acetonitrile solution of the one-electron reduced species, $[\text{Ru}^{\text{II}}(\text{trpy})(\text{L})(\text{NO}^*)]^{2+}$ ($[\mathbf{4}]^{2+}$) undergoes facile photorelease of NO over a period of ~ 30 min via the selective cleavage of the Ru–NO bond and with concomitant formation of the solvate species $[\text{Ru}^{\text{II}}(\text{trpy})(\text{L})(\text{CH}_3\text{CN})]^{2+}$ ($[\mathbf{2}]^{2+}$). The progression of the photocleavage of the Ru^{II}–NO[•] bond in $[\mathbf{4}]^{2+}$ was monitored spectrophotometrically in CH_3CN (Figure 11), and the presence of isosbestic points suggests the direct transformation of $[\text{Ru}^{\text{II}}(\text{trpy})(\text{L})(\text{NO}^*)]^{2+}$ ($[\mathbf{4}]^{2+}$) to $[\text{Ru}^{\text{II}}(\text{trpy})(\text{L})(\text{CH}_3\text{CN})]^{2+}$ ($[\mathbf{2}]^{2+}$). The rate of the first-order photolytic release of NO (k_{NO}) has been determined at $2.0 \times 10^{-1} \text{min}^{-1}$ ($t_{1/2} \approx 3.5$ min). The rate of photorelease of “NO” from the analogous complex $[\text{Ru}^{\text{II}}(\text{trpy})(\text{L}^4)(\text{NO}^*)]^{2+}$ (k_{NO} [min^{-1}] = 4.4×10^{-3} and $t_{1/2} \approx 157 \text{min}$ ^{7d}) is 45 times slower than that estimated for $[\mathbf{4}]^{2+}$.

(16) Ford, P. C.; Lorkovic, I. M. *Chem. Rev.* **2002**, *102*, 993.

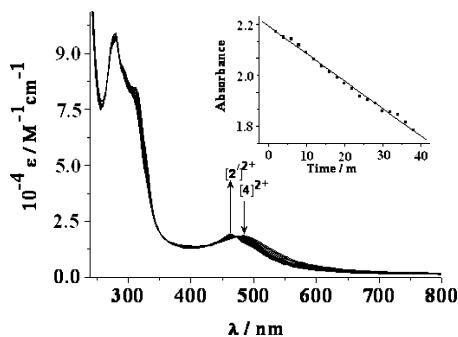


Figure 11. Time evolution of the electronic spectrum (2 min time intervals) of a solution of $[\text{Ru}(\text{trpy})(\text{L})(\text{NO})]^{2+}$ ($[\mathbf{4}]^{2+}$, 0.41×10^{-4} M) in CH_3CN under the exposure of light (Xe lamp, 350 W). The inset shows absorbance versus time plot at 488 nm corresponding to $[\mathbf{4}]^{2+}$.

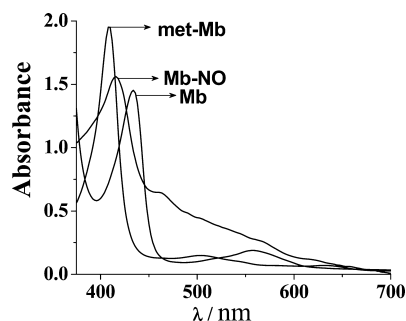


Figure 12. Absorption spectra of met-Mb, reduced Mb, and the Mb–NO adduct in water.

This sort of photolytic cleavage of an M–NO bond maintaining the overall integrity of the remaining part of the molecule is known to have biological significance.⁴ Therefore, the feasibility of binding the liberated “NO” to a biological target molecule such as myoglobin was explored.

When liberated “NO” from photolyzed $[\mathbf{4}]^{2+}$ in acetonitrile was passed through the aqueous solution of reduced Mb under deoxygenated condition the Mb–NO adduct was spontaneously formed. This has been evidenced via the development of a characteristic intense band of Mb–NO at $\lambda_{\text{max}} = 419$ nm (Figure 12).^{17,18} The small absorption at 462 nm in the spectrum of Mb–NO arises from the presence of the solvated species $[\text{Ru}^{\text{II}}(\text{trpy})(\text{L})(\text{CH}_3\text{CN})]^{2+}$ $[\mathbf{2}']^{2+}$ in the photolyzed solution.

Conclusion

The present work demonstrates that the combination of trpy and L coligands in the complex framework of $\{\text{Ru}(\text{trpy})(\text{L})(\text{NO})\}$ facilitates the stabilization of the nitrosyl group in both the NO^+ and NO^\bullet redox states which are reversibly interconvertible via one-electron transfer. The changes in $\{\text{RuNO}\}^{6,7}$ bonding for $[\mathbf{4}]^{3+}$ and $[\mathbf{4}]^{2+}$ are evident from the ca. 300 cm^{-1} shift in the $\nu(\text{NO})$ stretching frequency. The analysis of the EPR spectrum of $[\mathbf{4}]^{2+}$ suggests significant metal contributions to the NO-based SOMO. The NO^+ center in $[\mathbf{4}]^{3+}$ is sufficiently electrophilic to form the

corresponding nitro species $[\mathbf{3}]^+$ in the presence of OH^- . The oxidation of the radical species $[\mathbf{4}]^{2+}$ to $[\mathbf{4}]^{3+}$ in the presence of a steady flow of dioxygen proceeds through an associatively activated pathway with a pseudo-first-order rate constant of $5.33 \times 10^{-3} \text{ s}^{-1}$ at 298 K. In acetonitrile solution the Ru–NO bond in $[\mathbf{4}]^{2+}$ is susceptible to undergo photo-cleavage on exposure to light, forming the solvated species $[\mathbf{2}']^{2+}$. The liberated NO can be scavenged by myoglobin.

Experimental Section

Materials. The precursor complex $\text{Ru}(\text{trpy})\text{Cl}_3$ ¹⁹ and 2-phenylimidazo[4,5-*f*]1,10-phenanthroline (L)²⁰ were prepared as reported. 2,2':6',2''-Terpyridine and silver nitrate were purchased from Aldrich. Other chemicals and solvents were reagent grade and used as received. For spectroscopic studies HPLC grade solvents were used.

Instrumentation. Solution electrical conductivity was checked using a Systronic conductivity bridge 305. Infrared spectra were taken on a Nicolet spectrophotometer with samples prepared as KBr pellets. ¹H NMR spectra were recorded using a 300 MHz Varian FT spectrometer with $(\text{CD}_3)_2\text{SO}$ used as solvent. Cyclic voltammetric and coulometric measurements were carried out using a PAR model 273A electrochemistry system. A platinum wire working electrode, a platinum wire auxiliary electrode, and a saturated calomel reference electrode (SCE) were used in a standard three-electrode configuration. Tetraethylammoniumperchlorate (TEAP) was used as the supporting electrolyte and the solution concentration was ca. 10^{-3} M; the scan rate used was 50 mV s^{-1} . A platinum gauze working electrode was used in the coulometric experiments. All electrochemical experiments were carried out under dinitrogen atmosphere. IR spectroelectrochemical studies were performed in $\text{CH}_3\text{CN}/0.1 \text{ M Bu}_4\text{NPF}_6$ at 298 K using an optically transparent thin layer electrode (OTTLE) cell²¹ mounted in the sample compartment of a Perkin-Elmer 1760X FTIR instrument. The EPR measurements were made in a two-electrode capillary tube²² with a X-band Bruker system ESP300. UV–vis spectral studies were performed on a Perkin-Elmer Lambda 950 spectrophotometer. The elemental analyses were carried out with a Perkin-Elmer 240C elemental analyzer. Electrospray mass spectra were recorded on a Micromass Q-ToF mass spectrometer. Magnetic susceptibility was measured with a CAHN electrobalance 7550. Emission experiments were performed using a Perkin-Elmer LS55 luminescence spectrometer fitted with a cryostat.

Kinetic Experiment. For the determination of k in the conversion process of $[\text{Ru}^{\text{II}}(\text{trpy})(\text{L})(\text{NO}^+)]^{3+}$ ($[\mathbf{4}]^{3+}$) \rightarrow $[\text{Ru}^{\text{II}}(\text{trpy})(\text{L})(\text{NO}_2)]^+$ ($[\mathbf{3}]^+$) in acetonitrile in the presence of aqueous sodium hydroxide solution (pH \sim 10) the increase in absorbance (A_t) at 478 nm corresponding to λ_{max} of the nitro complex $[\mathbf{3}]^+$ was monitored as a function of time (t). A_α was measured when the intensity changes leveled off. Values of pseudo first order rate constants, k , were obtained from the slopes of linear least-squares plots of $-\ln(A_\alpha - A_t)$ against t . The activation parameters ΔH^\ddagger and ΔS^\ddagger were determined from the Eyring plot.²³

(17) (a) Fernandez, B. O.; Lorkovic, I. M.; Ford, P. C. *Inorg. Chem.* **2004**, *43*, 5393. (b) Patra, A. K.; Mascharak, P. K. *Inorg. Chem.* **2003**, *42*, 7363.

(18) SenGupta, N.; Basu, S.; Payra, P.; Mathur, P.; Lahiri, G. K.; Bhaduri, S. *Dalton Trans.* **2007**, 2594.

(19) Indelli, M. T.; Bignozzi, C. A.; Scandola, F.; Collin, J.-P. *Inorg. Chem.* **1998**, *37*, 6084.

(20) Liu, J. H.; Ren, X. Z.; Xu, H.; Huang, Y.; Liu, J. Z.; Ji, L. N.; Zhang, Q. L. *J. Inorg. Biochem.* **2003**, *95*, 194.

(21) Krejčík, M.; Danek, M.; Hartl, F. J. *Electroanal. Chem.* **1991**, *317*, 179.

(22) Kaim, W.; Ernst, S.; Kasack, V. *J. Am. Chem. Soc.* **1990**, *112*, 173.

(23) Wilkins, R. G. *The study of kinetics and mechanism of reaction of Transition Metal Complexes*; Allyn and Bacon: Boston, MA, 1974.

The pseudo-first-order rate constant for the conversion of $[\text{Ru}^{\text{II}}(\text{trpy})(\text{L})(\text{NO}^*)]^{2+}$ ($[\mathbf{4}]^{2+}$) \rightarrow $[\text{Ru}^{\text{II}}(\text{trpy})(\text{L})(\text{NO}^+)]^{3+}$ ($[\mathbf{4}]^{3+}$) in $\text{CH}_3\text{CN}/0.1 \text{ M HClO}_4$ solution in presence of steady flow of dioxygen was determined from the single-exponential fitting of the plot of change in absorbance against time at $\lambda_{\text{max}} = 488 \text{ nm}$. The activation parameters ΔH^\ddagger and ΔS^\ddagger were determined from the Eyring plot.²³

The first-order rate constant for the photorelease of NO from $[\text{Ru}^{\text{II}}(\text{trpy})(\text{L})(\text{NO}^*)]^{2+}$ ($[\mathbf{4}]^{2+}$) was determined from a single-exponential fitting of the plot of change in absorbance against time under photolysis condition at $\lambda_{\text{max}} = 488 \text{ nm}$ in acetonitrile.

Photoreleased NO Trapping by Myoglobin. A solution of $[\mathbf{4}](\text{ClO}_4)_2$ (3.0 mL) in acetonitrile was prepared in a quartz cuvette with an optical path length of 1 cm and sealed with a rubber septum. The solution was deoxygenated by purging with nitrogen gas and photolyzed for 30 min using a Xe 350 W lamp. The photoreleased free NO was allowed to pass through a solution of reduced myoglobin in water by a canula and the UV-vis spectrum was recorded.

Caution! Special precautions should be taken when handling perchloric acid and organic perchlorates.

Synthesis of $[\text{Ru}(\text{trpy})(\text{L})(\text{Cl})](\text{ClO}_4)$ ($[\mathbf{1}](\text{ClO}_4)$). The starting complex $[\text{Ru}(\text{trpy})\text{Cl}_3]$ (100 mg, 0.23 mmol), 2-phenylimidazo[4,5-*f*]1,10-phenanthroline (L) (67.19 mg, 0.227 mmol), excess LiCl (54 mg, 1.3 mmol), and NEt_3 (0.4 mL) were taken in 25 mL of ethanol, and the mixture was heated at reflux for 8 h under a dinitrogen atmosphere. The initial greenish solution gradually changed to deep purple. The solvent was then removed under reduced pressure. The dry mass thus obtained was dissolved in a minimum volume of acetonitrile, and an excess of a saturated aqueous solution of NaClO_4 was added. The solid precipitate thus obtained was filtered off and washed thoroughly with ice-cold water. The product was dried in vacuo over P_4O_{10} . It was then purified by using a silica gel column. The complex $[\mathbf{1}](\text{ClO}_4)$ was eluted by 2:1 CH_2Cl_2 - CH_3CN . Evaporation of the solvent under reduced pressure afforded pure $[\mathbf{1}](\text{ClO}_4)$. Yield: 118.28 mg (68%). Anal. Calcd for $\text{C}_{34}\text{H}_{23}\text{Cl}_2\text{N}_7\text{O}_4\text{Ru}$ (765.02) (found): C, 53.33 (53.01); H, 3.03 (2.96); N, 12.81 (12.79%). Molar conductivity $[\Lambda_{\text{M}} (\Omega^{-1} \text{ cm}^2 \text{ M}^{-1})]$ in acetonitrile: 147. $^1\text{H NMR}$ (CD_3) $_2\text{SO}$: $\delta = 10.29$ (d, 7.8 Hz, 1 H), 9.30 (d, 8.1 Hz, 1 H), 8.85 (d, 8.1 Hz, 2 H), 8.72 (t, 5.1 Hz, 2.7 Hz, 3 H), 8.59 (s, 1 H), 8.23 (m, 3 H), 7.94 (t, 7.2 Hz, 7.5 Hz, 2 H), 7.64 (m, 4 H), 7.51 (m, 3 H), 7.23 (t, 6.6 Hz, 6.6 Hz, 2 H) ppm.

Synthesis of $[\text{Ru}(\text{trpy})(\text{L})(\text{H}_2\text{O})](\text{ClO}_4)_2$ ($[\mathbf{2}](\text{ClO}_4)_2$). The chloro complex $[\mathbf{1}](\text{ClO}_4)$ (100 mg, 0.130 mmol) was taken in 25 mL of water and heated at reflux for 10 min. An excess of AgNO_3 (221 mg, 1.3 mmol) was added to the hot solution and the heating was continued for 1.5 h. It was then cooled and the precipitated AgCl was separated by filtration through a sintered glass crucible (G-4). The volume of the filtrate was reduced to 10 mL and an excess of a saturated aqueous solution of NaClO_4 was added. The solid aqua complex $[\mathbf{2}](\text{ClO}_4)_2$ thus obtained was filtered off, washed with ice-cold water and dried in vacuo over P_4O_{10} . Yield: 86.24 mg (78%). Anal. Calcd for $\text{C}_{34}\text{H}_{25}\text{Cl}_2\text{N}_7\text{O}_9\text{Ru}$ (847.01) (found): C, 48.18 (47.97); H, 2.97 (3.11); N, 11.57 (11.27%). Molar conductivity $[\Lambda_{\text{M}} (\Omega^{-1} \text{ cm}^2 \text{ M}^{-1})]$ in acetonitrile: 240. $^1\text{H NMR}$ (CD_3) $_2\text{SO}$: $\delta = 9.37$ (m, 1 H), 8.95 (m, 3 H), 8.76 (q, 6.3 Hz, 9.3 Hz, 8.7 Hz, 3 H), 8.45 (m, 1 H), 8.32 (m, 3 H), 8.03 (m, 2 H), 7.64 (m, 7 H), 7.36 (m, 2 H) ppm.

Synthesis of $[\text{Ru}(\text{trpy})(\text{L})(\text{CH}_3\text{CN})](\text{ClO}_4)_2$ ($[\mathbf{2}'](\text{ClO}_4)_2$). The complex $[\mathbf{2}'](\text{ClO}_4)_2$ was prepared following the same procedure as stated above for $[\mathbf{2}](\text{ClO}_4)_2$, except using CH_3CN as solvent instead of water. Yield: 84.03 mg (74%). Anal. Calcd for $\text{C}_{36}\text{H}_{26}\text{Cl}_2\text{N}_8\text{O}_8\text{Ru}$ (870.02) (found): C, 49.65 (49.77); H, 3.01

(2.98); N, 12.88 (12.56%). Molar conductivity $[\Lambda_{\text{M}} (\Omega^{-1} \text{ cm}^2 \text{ M}^{-1})]$ in acetonitrile: 236. $^1\text{H NMR}$ (CD_3) $_2\text{SO}$: $\delta = 9.96$ (d, 4.8 Hz, 1 H), 9.4 (d, 8.4 Hz, 1 H), 8.96 (d, 8.4 Hz, 2 H), 8.88 (d, 7.8 Hz, 1 H), 8.78 (d, 8.4 Hz, 2 H), 8.5 (t, 8.4 Hz, 7.8 Hz, 2 H), 8.32 (d, 7.2 Hz, 2 H), 8.08 (t, 6.9 Hz, 7.5 Hz, 2 H), 7.69 (m, 7 H), 7.34 (t, 6.3 Hz, 6.3 Hz, 2 H) ppm.

Synthesis of $[\text{Ru}(\text{trpy})(\text{L})(\text{NO}_2)](\text{ClO}_4)$ ($[\mathbf{3}](\text{ClO}_4)$). The aqua complex $[\mathbf{2}](\text{ClO}_4)_2$ (100 mg, 0.118 mmol) was dissolved in 25 mL of hot water and an excess of NaNO_2 (194 mg, 2.81 mmol) was added. The mixture was heated at reflux for 1.5 h. The deep red solution of the aqua species changed to deep orange during the course of reaction. The pure crystalline nitro complex precipitated during cooling to room temperature. The solid $[\mathbf{3}](\text{ClO}_4)$ thus obtained was filtered off, washed with ice-cold water and dried in vacuo over P_4O_{10} . Yield: 76.91 mg (84%). Anal. Calcd for $\text{C}_{34}\text{H}_{23}\text{ClN}_8\text{O}_6\text{Ru}$ (776.04) (found): C, 52.57 (53.17); H, 2.99 (2.99); N, 14.44 (14.44%). Molar conductivity $[\Lambda_{\text{M}} (\Omega^{-1} \text{ cm}^2 \text{ M}^{-1})]$ in acetonitrile: 127. $^1\text{H NMR}$ (CD_3) $_2\text{SO}$: $\delta = 10.01$ (d, 5.1 Hz, 1 H), 9.32 (d, 8.1 Hz, 1 H), 8.85 (t, 8.4 Hz, 6.9 Hz, 3 H), 8.71 (d, 8.1 Hz, 2 H), 8.40 (m, 4 H), 8.01 (t, 8.1 Hz, 7.8 Hz, 2 H), 7.59 (m, 7 H), 7.28 (t, 6.6 Hz, 6.0 Hz, 2 H) ppm.

$[\text{Ru}(\text{trpy})(\text{L})(\text{NO})](\text{ClO}_4)_3$ ($[\mathbf{4}](\text{ClO}_4)_3$). Concentrated HNO_3 (2 mL) was added dropwise at 273 K on the solid nitro complex $[\mathbf{3}](\text{ClO}_4)$ (100 mg, 0.129 mmol) under stirring condition. To the pasty mass thus obtained was added an ice-cold concentrated HClO_4 solution (6 mL) with constant stirring. Addition of a saturated aqueous NaClO_4 solution resulted in a yellow precipitate which was filtered and washed with about 4 mL of ice-cold water and then dried in vacuo over P_4O_{10} . Yield: 101.22 mg (82%). Anal. Calcd for $\text{C}_{34}\text{H}_{23}\text{Cl}_3\text{N}_8\text{O}_{13}\text{Ru}$ (957.94) (found): C, 42.59 (41.39); H, 2.42 (2.42); N, 11.69 (10.99%). Molar conductivity $[\Lambda_{\text{M}} (\Omega^{-1} \text{ cm}^2 \text{ M}^{-1})]$ in acetonitrile: 314. $^1\text{H NMR}$ (CD_3) $_2\text{SO}$: 9.83 (d, 5.4 Hz, 1 H), 9.66 (d, 9.0 Hz, 1 H), 9.28 (m, 3 H), 9.16 (t, 6.9 Hz, 9.3 Hz, 1 H), 9.04 (d, 8.1 Hz, 2 H), 8.70 (t, 8.1 Hz, 5.1 Hz, 1 H), 8.49 (t, 7.8 Hz, 8.1 Hz, 2 H), 8.33 (d, 7.2 Hz, 2 H), 7.89 (m, 3 H), 7.63 (m, 6 H) ppm.

Synthesis of $[\text{Ru}(\text{trpy})(\text{L})(\text{NO})](\text{ClO}_4)_2$ ($[\mathbf{4}](\text{ClO}_4)_2$). The nitroso complex $[\mathbf{4}](\text{ClO}_4)_3$ (100 mg, 0.116 mmol) was dissolved in 5 mL of CH_3CN , and excess hydrazine hydrate was added under stirring over a period of 5 min under a dinitrogen atmosphere. The stirring was continued at room temperature for further 0.5 h. The initially yellow solution of $[\mathbf{4}](\text{ClO}_4)_3$ changed to red-brown. The solvent was then removed under reduced pressure and the solid mass thus obtained was washed with little ice-cold water and then dried in vacuo over P_4O_{10} . Yield: 65.4 mg (73%). Anal. Calcd for $\text{C}_{34}\text{H}_{23}\text{Cl}_2\text{N}_8\text{O}_9\text{Ru}$ (859.00) (found): C, 47.51 (47.42); H, 2.70 (2.81); N, 13.04 (12.93%). Molar conductivity $[\Lambda_{\text{M}} (\Omega^{-1} \text{ cm}^2 \text{ M}^{-1})]$ in acetonitrile: 215. Magnetic moment, $\mu(\text{B.M.})$ at 298 K = 1.83. For other physical characterizations, see main text.

Crystallography. Single crystals of $[\mathbf{1}](\text{ClO}_4) \cdot 4.5\text{H}_2\text{O}$, $[\mathbf{2}'-\text{H}^+](\text{ClO}_4)_3 \cdot \text{H}_2\text{O}$ and $[\mathbf{4}-\text{H}^+](\text{ClO}_4)_4 \cdot 2\text{H}_2\text{O}$ were grown by slow evaporation of the respective 1:1 acetonitrile-benzene solutions at 298 K in air. X-ray data were collected using an OXFORD XCALIBUR-S CCD single crystal X-ray diffractometer. The structures were solved and refined by full-matrix least-squares techniques on F^2 using the SHELX-97 program.²⁴ The absorption corrections were done by the multiscan technique. All data were corrected for Lorentz and polarization effects, and the nonhydrogen atoms were refined anisotropically. Hydrogen atoms were included in the refinement process as per the riding model.

Acknowledgment. Financial support received from the Department of Science and Technology (DST) and Council of

Scientific and Industrial Research (CSIR), New Delhi (India), the DAAD, the DFG, and the FCI (Germany) is gratefully acknowledged. Special acknowledgement is made to the Sophisticated Analytical Instrument Facility (SAIF), Indian Institute of Technology, Bombay, for providing the NMR facility.

(24) Sheldrick, G. M. *Program for Crystal Structure Solution and Refinement*; Universität Göttingen: Göttingen, Germany, 1997.

Supporting Information Available: Crystallographic parameters of [1](ClO₄)·4.5H₂O, [2'-H⁺](ClO₄)₃·H₂O, and [4-H⁺](ClO₄)₄·2H₂O (Table S1); selected bond distances and angles of [1](ClO₄)·4.5H₂O, [2'-H⁺](ClO₄)₃·H₂O, and [4-H⁺](ClO₄)₄·2H₂O (Table S2); ¹H NMR spectra of [1](ClO₄), [2](ClO₄)₂, [2'](ClO₄)₂, [3](ClO₄), and [4](ClO₄)₃ in (CD₃)₂SO (Figure S1); EPR spectrum of [2']³⁺ in CH₃CN (Figure S2). This material is available free of charge via the Internet at <http://pubs.acs.org>.

IC702160W